Accurate Insertion Loss Measurements of the Juno Patch Array Antennas

Neil Chamberlain, Jacqueline Chen, Richard Hodges

Jet Propulsion Laboratory, California Institute of Technology
4800 Oak Grove Drive
Pasadena, CA 91109

John Demas

Nearfield Systems Inc.
19730 Magellan Drive
Torrance, CA 90502

Abstract—*This paper describes two independent methods for estimating the insertion loss of patch array antennas that were developed for the Juno Microwave Radiometer instrument. One method is based principally on pattern measurements while the other method is based solely on network analyzer measurements. The methods are accurate to within 0.1 dB for the measured antennas and show good agreement (to within 0.1dB) of separate radiometric measurements.*

1. Introduction

This paper discusses the calculation of insertion loss in the Juno Microwave Radiometer patch array antennas [1]. Two different methods are presented for calculating the loss from measurements that are accurate to within 0.1 dB. This accuracy, it is claimed, is better than what is typically obtained from pattern measurements in a good antenna range. The first method uses a curve fit to frequency-dependent loss calculations inferred from pattern measurements. The second method relies on estimating losses separately for the antenna feed network and the antenna element, and adding the two. While these methods are not applicable to all antennas, the approaches outlined here have applicability to a broad class of corporate-fed array antennas where the general nature of the loss-frequency characteristic is well understood.

2. Method 1: Pattern Measurements

Antenna insertion loss in the first method is measured indirectly by subtracting the directivity of measured pattern data from measured gain.

These measurements are performed at room temperature and therefore produce worst case loss estimates, as it is known that losses decrease at the lower operating temperatures of the antennas. Gain is calculated using the substitution method from a standard gain horn measurement. The far-fields of the AUT and standard gain horn (SGH) are first measured. Equation 1 can be used to compute the gain of the AUT (not in dB):

$$G_{AUT} = \left|\frac{E_{AUT}}{E_{SGH}}\right|^2 \frac{G_{SGH}}{1-\left|\Gamma_{AUT}\right|^2} \tag{1}$$

where G_{SGH} is the gain of the gain standard, E_{SGH} is the maximum far-field field strength of the standard gain horn, E_{AUT} is the maximum far-field field strength of the AUT, and Γ_{AUT} is the measured reflection coefficient of the AUT.

The gain of the SGH is estimated by computing the directivity from measured data and then adding a theoretically-derived loss. At the frequency of operation of the antennas, surface roughness and irregularities can be ignored and the theoretical attenuation is a good estimate of the actual loss. The attenuation in the flared part of the gain horn antenna is predicted from attenuation in a rectangular waveguide. In any case the losses are on the order of a few thousandths of a dB and do not significantly affect the gain calculation.

Using the measured directivity of the gain standard antenna to estimate its gain results in a net reduction in uncertainty of the calculated AUT gain because the peak far-field strength of the gain standard essentially factors out. Equation 2 shows that the AUT gain depends on the measured AUT maximum far-field strength, the integrated measured gain standard far-field strength, the measured AUT reflection loss and estimated gain standard loss, L_{SGH}.

$$G_{AUT} = \frac{4\pi |E_{AUT}|^2}{\iint |E_{SGH}(\theta,\phi)|^2 \sin\theta d\theta d\phi} \left\{ \frac{1}{L_{SGH}\left(1-|\Gamma_{AUT}|^2\right)} \right\} \quad (2)$$

The AUT insertion loss is calculated as the ratio of estimated directivity and gain:

$$L_{AUT} = D_{AUT} / G_{AUT} \quad (3)$$

$$L_{AUT} = \frac{\iint |E_{SGH}(\theta,\phi)|^2 \sin\theta d\theta d\phi}{\iint |E_{AUT}(\theta,\phi)|^2 \sin\theta d\theta d\phi} L_{SGH}\left(1-|\Gamma_{AUT}|^2\right) \quad (4)$$

Equation 4 is equivalent to Equation 3 substituted by Equation 1, with the assumption that the SGA gain is computed based on the measured directivity and estimated loss. The principal sources of error in the loss calculation are the integrated measurements of E_{AUT} and E_{SGH}, assuming that the AUT reflection loss can be measured accurately and the gain standard loss can be estimated accurately (or is insignificant). The resulting uncertainty can be reduced further by curve fitting the loss estimates from the above equation to a quadratic polynomial. The resulting fitted loss tracks the measured insertion loss of the feed, the latter being the dominant component of the overall insertion loss (Figures 1 and 2).

3. Method 2: Network Analyzer Measurements

The second method uses a vector network analyzer to measure the S-parameters of the antenna feed network and antenna element separately. This method is generally easier (and cheaper) than the first method because it avoids pattern measurements. It is assumed that the antenna is configured in such a way that the feed network is (at some point) separable from the antenna elements. This is naturally the case for antennas such as corporate-fed patch arrays, but not the case for antennas such as slot arrays.

The insertion loss for the feed network is estimated from measurements of N-port scattering parameters of the feed network. For large feed networks, this calculation can be performed by making S-parameter measurements of feed subassemblies and then calculating the total feed S-parameters in a network model.

$$L_{feed}(f) = -10\log_{10}\left\{\sum_{n=2}^{N} |S_{1n}(f)|^2\right\} + 10 * \log_{10}\left\{1-|S_{11}(f)|^2\right\} \quad (5)$$

The loss of the antenna element is inferred from a return loss measurement of an isolated element that is not connected to the feed. It relies on an accurate estimate of the reflection coefficient of the lossless antenna element (say from a modeling program such as HFSS) and an accurate measurement of the reflection coefficient of the array element. Additionally, the loss mechanism in array element should be well understood. In Equation 6, it is assumed that losses are dominated by skin effect losses and other losses are negligible. The array element insertion loss is estimated as the loss that minimized the mean error between the lossless reflection coefficient estimate (from modeling software) and reflection coefficient measurement of the element:

$$\underset{\min}{L_{element}} \left\langle \left| \left| S_{11}^{MOD}(f) 10^{-2L_{element}\sqrt{f/f_0}/20} \right|^2 - \left| S_{11}^{MEAS}(f) \right|^2 \right| \right\rangle \quad (6)$$

Where $\langle\,\rangle$ indicates taking the mean of the enclosed quantities over frequency and where $\sqrt{f/f_0}$ expresses the frequency-dependent skin-effect loss relative to the center frequency.

These methods are verified for two different patch array antennas operating at 600 MHz and 1250 MHz respectively.

4. Method 1: Results

Figure 1 and Figure 2 show gain, directivity, and loss measurements for the two patch array antennas. These antennas are named A1 (600 MHz) and A2 (1250 MHz). The A2 antenna was measured on two separate occasions. Measured directivity is computed by integrating measured antenna patterns. These values agree well (to within 0.1 dB) with the directivity computed from modeled antenna patterns. The measured gain is computed using Equation 1 and is plotted in the left hand graph of each figure. Loss is calculated by subtracting the measured gain from measured directivity (equivalently Equation 3) and is plotted as the blue curve in the right hand graph of each figure. These calculations are tabulated in Table 1.

Each of the terms in the calibration equation contributes to the overall uncertainty in the gain estimate. The error in the loss estimate is evident in the 'scatter' in the data of in the above figures. A second-order polynomial fit is made to the measured and is plotted as the magenta curve in the right hand graphs. The rationale for this fit is as follows. The overall loss in the antenna is composed of two parts: the loss in the feed network and the loss in the antenna element. The feed network loss has a quadratic characteristic due to the resonant Wilkinson circuits that make provide the power splitting in the feed. A second order fit to the measured loss data produces a curve that closely tracks the loss of the feed, which dominates the overall loss.

5. Method 2: Results

Reflection coefficient measurements for the two isolated antenna elements are in Figure 3. These responses are detuned from their design frequencies of 600 MHz and 1250 MHz because the elements are not in their respective array

environments. The HFSS simulations employ the corresponding boundary conditions. The frequency agreement between the modeled and measured reflection coefficients is good because of the high accuracy of the HFSS modeling software. This due in part to the fact that the antenna elements contain no dielectric (therefore the uncertainty due to modeling dielectric materials is avoided) and also to the fact that a single element can be meshed very accurately in HFSS.

The estimated loss (at center frequency) is 0.22 dB for A1 and 0.10 dB for A2. The loss is lower for the higher frequency antenna because the dimensions of the element are approximately half of the low frequency element, but skin effect losses increase as the square root of frequency (from a simple scaling calculation, this would result in the A2 loss being 0.15 dB). Insertion loss data (derived from measurements of the feed assemblies) are shown in Table 1. The loss estimates at the maximum operating frequency of each antenna are summarized as follows:

A1 insertion loss (at 0.615 GHz)

- Method 1 (Pattern Measurements): 1.04 dB
- Method 2 (Loss Measurements):
  - Feed insertion loss: 0.935 dB
  - Patch insertion loss: 0.223 dB
  - Total: 1.16 dB
- Average of Method 1 and Method 2: 1.10 dB
- Uncertainty: ±0.1 dB

A2 insertion loss (at 1.280 GHz)

- Method 1 (Pattern Measurements):
  - Measurement 1: 1.19 dB
  - Measurement 2: 1.31 dB
- Method 2 (Loss Measurements):
  - Feed insertion loss: 1.042 dB
  - Patch insertion loss: 0.103 dB
  - Total: 1.14 dB
- Average of Method 1 and Method 2: 1.21 dB
- Uncertainty: ±0.1 dB

Overall, the loss of the A2 antenna is slightly higher than the loss of the A1 antenna, the former being 1.21 dB at 1.28 GHz versus 1.10 dB at 615 MHz. Various factors contribute to make the losses deviate from the reduction by 0.7 that would be predicated from frequency scaling, including the fact that some items (such as the connectors) are the same for A2 as A1, and other items (notably the coaxial cables) are proportionally longer for A2.

6. Conclusions

Two independent methods for calculating the insertion loss of the Juno Microwave Radiometer patch arrays have been presented. Generally the loss calculations are found to agree 0.2dB and the claimed accuracy is ±0.1 dB. Separate radiometric measurements of the A1 antenna agree to within 0.1dB of the above estimates.

References

[1] N. Chamberlain, J. Chen, R. Hodges, R. Hughes, J. Jakoboski, *Juno Microwave Radiometer All-Metal Patch Array Antennas*, IEEE APS Conference, Toronto, Canada, 2010

Acknowledgements

The research described in this paper was carried out at the Jet Propulsion Laboratory, California Institute of Technology, under a contract with the National Aeronautics and Space Administration. Reference herein to any specific commercial product, process, or service by trade name, trademark, manufacturer, or otherwise, does not constitute or imply its endorsement by the United States Government or the Jet Propulsion Laboratory, California Institute of Technology.

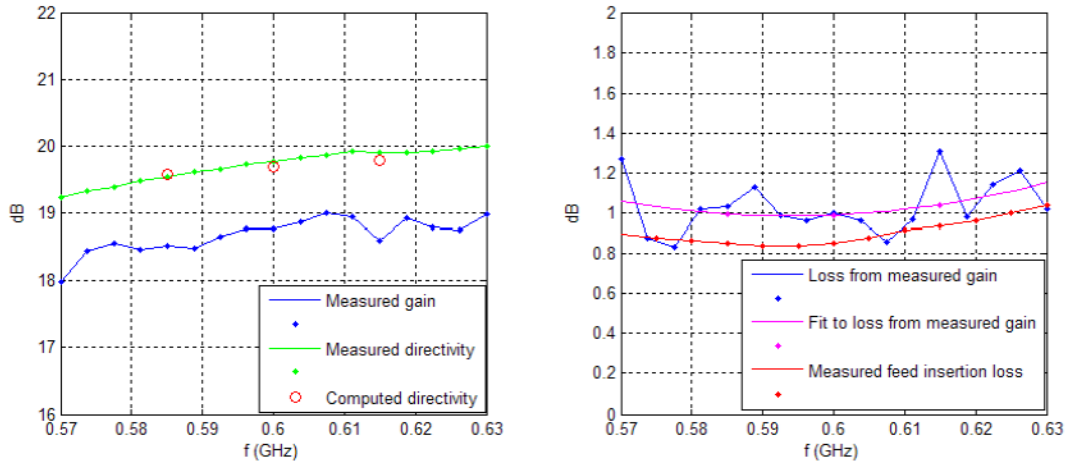

Figure 1. Measured gain and directivity (left) and derived loss (right) for A1.

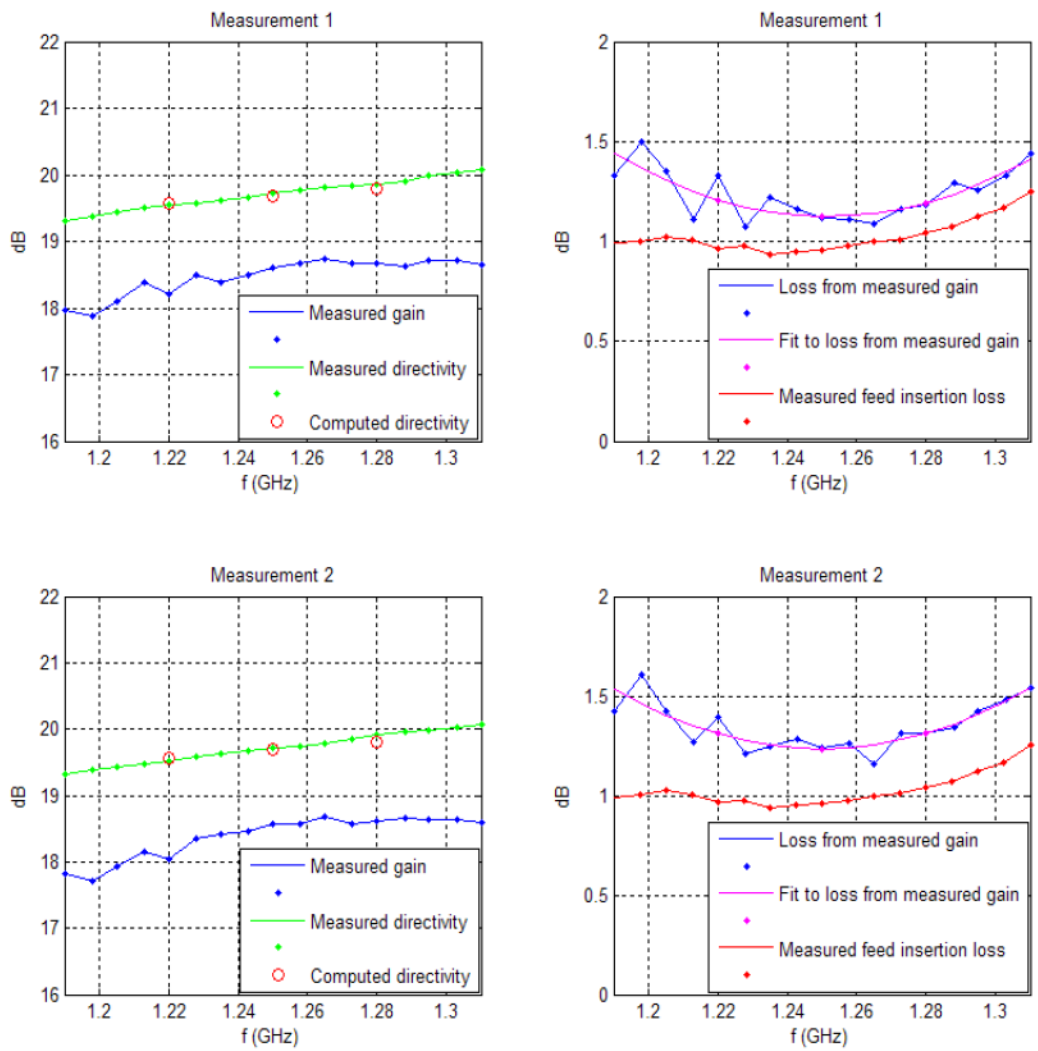

Figure 2. Measured gain and directivity (left) and measured loss (right) for A2: pre-environmental test data (top), post-environmental test data (bottom).

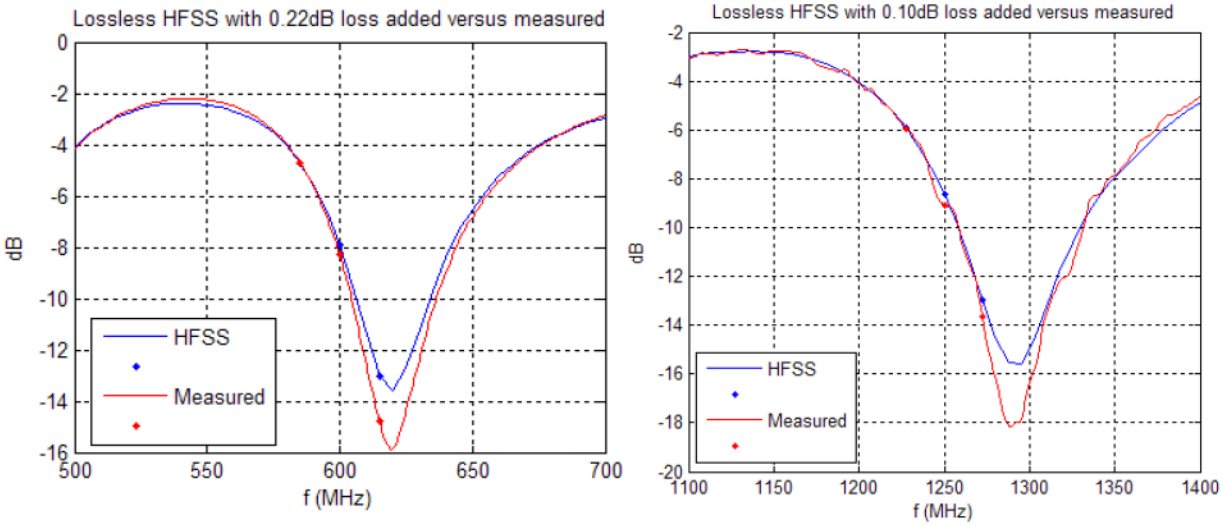

Figure 3. Reflection coefficient measurements compared to HFSS predications: isolated A1 antenna element (left) and A2 antenna element (right).

f	D_{AUT}	G_{SGH}	$\lvert E_{AUT}\rvert^2$	$\lvert E_{SGH}\rvert^2$	$1-\lvert S_{11}\rvert^2$	G_{AUT}	L_{AUT}	L'_{AUT}	L_{feed}
Freq	Dir	Gain SGH	Max FF AUT	Max FF SGH	Loss	Gain AUT	Loss AUT	Fit Loss AUT	Loss Feed
(GHz)	(dBi)	(dBi)	(dB)	(dB)	(dB)	(dBi)	(dB)	(dB)	(dB)
0.570	19.24	15.18	20.65	17.93	0.49	17.97	1.27	1.06	0.90
0.574	19.32	15.27	21.05	18.28	0.40	18.44	0.88	1.04	0.88
0.577	19.39	15.35	21.44	18.54	0.31	18.56	0.83	1.02	0.87
0.581	19.48	15.42	21.60	18.77	0.21	18.46	1.02	1.01	0.86
0.585	19.54	15.50	21.90	19.03	0.15	18.51	1.03	1.00	0.85
0.589	19.61	15.56	22.03	19.19	0.08	18.48	1.13	0.99	0.84
0.592	19.65	15.62	22.60	19.61	0.04	18.66	0.99	0.99	0.84
0.596	19.73	15.68	22.71	19.63	0.01	18.77	0.96	0.99	0.85
0.600	19.77	15.69	22.92	19.84	0.00	18.77	1.00	0.99	0.86
0.604	19.83	15.71	23.12	19.99	0.03	18.87	0.96	1.00	0.87
0.608	19.86	15.72	23.10	19.90	0.08	19.00	0.86	1.01	0.89
0.611	19.92	15.76	23.36	20.32	0.15	18.95	0.97	1.02	0.91
0.615	19.91	15.85	22.97	20.42	0.20	18.60	1.31	1.04	0.94
0.619	19.91	15.90	23.38	20.57	0.21	18.93	0.98	1.06	0.96
0.623	19.92	15.98	23.35	20.77	0.22	18.78	1.14	1.09	0.99
0.626	19.96	16.05	23.15	20.68	0.23	18.75	1.21	1.12	1.01
0.630	20.01	16.06	23.49	20.83	0.27	18.99	1.02	1.15	1.03

Table 1. Loss calculation from pattern measurements